Observation of the Decays $\Lambda_b^0 \to \chi_{c1} p K^-$ and $\Lambda_b^0 \to \chi_{c2} p K^-$

R. Aaij *et al.*[*]
(LHCb Collaboration)

(Received 27 April 2017; published 8 August 2017)

The first observation of the decays $\Lambda_b^0 \to \chi_{c1} p K^-$ and $\Lambda_b^0 \to \chi_{c2} p K^-$ is reported using a data sample corresponding to an integrated luminosity of 3.0 fb^{-1}, collected by the LHCb experiment in pp collisions at center-of-mass energies of 7 and 8 TeV. The following ratios of branching fractions are measured:

$$\frac{\mathcal{B}(\Lambda_b^0 \to \chi_{c1} p K^-)}{\mathcal{B}(\Lambda_b^0 \to J/\psi p K^-)} = 0.242 \pm 0.014 \pm 0.013 \pm 0.009,$$
$$\frac{\mathcal{B}(\Lambda_b^0 \to \chi_{c2} p K^-)}{\mathcal{B}(\Lambda_b^0 \to J/\psi p K^-)} = 0.248 \pm 0.020 \pm 0.014 \pm 0.009,$$
$$\frac{\mathcal{B}(\Lambda_b^0 \to \chi_{c2} p K^-)}{\mathcal{B}(\Lambda_b^0 \to \chi_{c1} p K^-)} = 1.02 \pm 0.10 \pm 0.02 \pm 0.05,$$

where the first uncertainty is statistical, the second systematic, and the third due to the uncertainty on the branching fractions of the $\chi_{c1} \to J/\psi\gamma$ and $\chi_{c2} \to J/\psi\gamma$ decays. Using both decay modes, the mass of the Λ_b^0 baryon is also measured to be $m_{\Lambda_b^0} = 5619.44 \pm 0.28 \pm 0.26$ MeV/c^2, where the first and second uncertainties are statistical and systematic, respectively.

DOI: 10.1103/PhysRevLett.119.062001

Since the birth of the quark model, it has been speculated that hadrons could be formed from multiquark states beyond the well-studied quark-antiquark (meson) and three-quark (baryon) combinations [1–3]. Using a six-dimensional amplitude analysis of the $\Lambda_b^0 \to J/\psi p K^-$ decay mode, the LHCb Collaboration observed the $P_c(4380)^+$ and $P_c(4450)^+$ states [4,5], which are consistent with $uudc\bar{c}$ hidden-charm pentaquarks decaying to $J/\psi p$. Many phenomenological models describing the dynamics of these states have been proposed, including meson-baryon molecules [6–8], compact pentaquarks [9–11], and kinematic rescattering effects [12–16]. In particular, the authors of Ref. [12] noted the closeness of the $P_c(4450)^+$ mass to the $\chi_{c1} p$ threshold and proposed that, if the $P_c(4450)^+$ state is a rescattering effect, then it would not appear as an enhancement near the $\chi_{c1} p$ threshold in the $\Lambda_b^0 \to \chi_{c1} p K^-$ decay mode, an approach recently challenged in Ref. [17]. This Letter presents an initial stage in the investigation of this hypothesis by making the first observation of $\Lambda_b^0 \to \chi_{c1} p K^-$ and $\Lambda_b^0 \to \chi_{c2} p K^-$ decays and measurements of their branching fractions relative to the $\Lambda_b^0 \to J/\psi p K^-$ decay. Throughout this Letter, the inclusion of charge-conjugated processes is implied and the symbol χ_{cJ} is used to denote the χ_{c1} and χ_{c2} states collectively. All Λ_b^0 decay modes considered here proceed via the same quark-level process, whose dominant contribution is shown in Fig. 1. A measurement of the Λ_b^0 baryon mass is also presented.

Previous measurements of the branching fractions of $B \to \chi_{cJ} K$ decays [18–20] have shown that the χ_{c2} mode is suppressed relative to the χ_{c1} mode, in agreement with the predictions from the factorization approach [21], although the suppression appears to be lessened when additional particles are present in the final state [22]. Studying the production of χ_{cJ} mesons in Λ_b^0 baryon decays will help to further test the factorization approach, as the additional spectator quark in the baryon decay may play an important role in modifying final-state interactions.

The measurements described in this Letter are based on a data sample corresponding to 1.0 fb^{-1} of integrated luminosity collected by the LHCb experiment in pp collisions at a center-of-mass energy of 7 TeV in 2011, and 2.0 fb^{-1} at 8 TeV in 2012. The LHCb detector [23,24] is a single-arm forward spectrometer covering the pseudorapidity range $2 < \eta < 5$, designed for the study of particles containing b

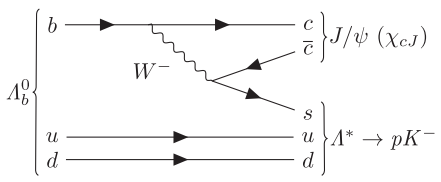

FIG. 1. Feynman diagram of $\Lambda_b^0 \to J/\psi \Lambda^*$ and $\Lambda_b^0 \to \chi_{cJ} \Lambda^*$ decays, where Λ^* refers to an excited Λ baryon.

[*]Full author list given at the end of the article.

or c quarks. The detector includes a high-precision tracking system consisting of a silicon-strip vertex detector surrounding the pp interaction region, a large-area silicon-strip detector located upstream of a dipole magnet with a bending power of about 4 Tm, and three stations of silicon-strip detectors and straw drift tubes placed downstream of the magnet. The tracking system provides a measurement of momentum, p, of charged particles with a relative uncertainty that varies from 0.5% at low momentum to 1.0% at 200 GeV/c. The minimum distance of a track to a primary vertex (PV), the impact parameter (IP), is measured with a resolution of $(15 + 29/p_{\mathrm{T}})$ μm, where p_{T} is the component of the momentum transverse to the beam, in GeV/c. Different types of charged hadrons are distinguished using information from two ring-imaging Cherenkov detectors. Photons, electrons, and hadrons are identified by a calorimeter system consisting of scintillating-pad and preshower detectors, an electromagnetic calorimeter, and a hadronic calorimeter. Muons are identified by a system composed of alternating layers of iron and multiwire proportional chambers. The online event selection is performed by a trigger, which consists of a hardware stage, based on information from the calorimeter and muon systems, followed by a software stage, which applies a full event reconstruction. The software trigger selects events that contain a pair of oppositely charged muons that form a vertex that is significantly separated from all PVs.

In the simulation, pp collisions are generated using Pythia 8[25] with a specific LHCb configuration [26]. Decays of hadronic particles are described by EvtGen [27], in which final-state radiation is generated using PHOTOS [28]. The interaction of the generated particles with the detector, and its response, are implemented using the Geant4 toolkit [29] as described in Ref. [30]. The products of the Λ_b^0 decays are generated uniformly within the available phase space.

The $\Lambda_b^0 \to \chi_{cJ} p K^-$ and $\Lambda_b^0 \to J/\psi p K^-$ candidates are reconstructed via the decays $\chi_{cJ} \to J/\psi\gamma$ and $J/\psi \to \mu^+\mu^-$. To separate signal from background, an offline selection is applied after the trigger, consisting of a loose preselection followed by a multivariate classifier based on a gradient-boosted decision tree (GBDT) [31].

The J/ψ candidates are formed from two oppositely charged particles with $p_{\mathrm{T}} > 550$ MeV/c, identified as muons and consistent with originating from a common vertex, but inconsistent with originating from any PV. The invariant mass of the $\mu^+\mu^-$ pair is required to be in the range $[3000, 3170]$ MeV/c^2. The χ_{cJ} candidates are formed from a J/ψ candidate and a photon with $p_{\mathrm{T}} > 700$ MeV/c. Photons that are consistent with originating from a π^0 meson when combined with any other photon in the event are removed. The invariant mass of the $\mu^+\mu^-\gamma$ combination is required to be in the range $[3400, 3700]$ MeV/c^2. In the following, the notation $[c\bar{c}]$ will be used to refer to the initial J/ψ or χ_{cJ} candidate from the Λ_b^0 baryon decay, while the notation $m(J/\psi X)$ or $m(\chi_{cJ} X)$ denotes an invariant mass that has been calculated with a mass constraint applied to the J/ψ or χ_{cJ} candidate.

The Λ_b^0 candidates are formed from a $[c\bar{c}]$ candidate and two good-quality oppositely charged tracks each with $p_{\mathrm{T}} > 200$ MeV/c, identified as a proton and kaon. Both tracks are required to be significantly displaced from any PV. A kinematic fit [32] is applied to the Λ_b^0 candidate, with the J/ψ and χ_{c1} masses constrained to their known values [33], and the Λ_b^0 candidate constrained to point back to a PV. This has the effect of producing separated peaks for the two decay modes. The mass resolution for $\Lambda_b^0 \to \chi_{c2} p K^-$ decays is lower compared to that for $\Lambda_b^0 \to \chi_{c1} p K^-$ decays due to the wrong mass hypothesis of the $[c\bar{c}]$ candidate.

Contributions from $B^0 \to [c\bar{c}] K^+\pi^-$ ($B_s^0 \to [c\bar{c}]\phi$, $\phi \to K^+K^-$) decays, where the π^- (K^-) is misidentified as an antiproton, are suppressed by placing tighter particle identification requirements on the misidentified hadron for candidates with an invariant mass within 30 MeV/c^2 of the B^0 (B_s^0) mass [33] when evaluated using π^- or K^- mass assignments for the antiproton candidates. Typical misidentification probabilities are 5%–15%, dependent on the particle momentum [34]. In the $\Lambda_b^0 \to \chi_{cJ} p K^-$ samples, small contributions from $B^0 \to J/\psi K^+\pi^-$ or $B_s^0 \to J/\psi\phi$ decays, where in addition to the misidentification the J/ψ meson is combined with a random photon in the event, are removed by the requirement that $m(J/\psi K^+\pi^-)$ or $m(J/\psi K^+K^-)$ are within 30 MeV/c^2 of the B^0 or B_s^0 mass. Additionally, $\phi \to K^+K^-$ decays are vetoed by removing all candidates where the invariant mass of the pK^- combination is within 12 MeV/c^2 of the known ϕ meson mass when the kaon mass is used instead of the proton mass. Further misreconstructed backgrounds are studied using a fast simulation package [35] and are found to have no peaking components in the invariant mass window of interest.

The GBDT is used to further suppress the combinatorial background. It is trained on a simulated sample of $\Lambda_b^0 \to \chi_{c1} p K^-$ decays for the signal and candidates from data with $m(\chi_{c1} p K^-)$ in the range $[5700, 5800]$ MeV/c^2 for the background. Twelve variables are used as input. The first of these is the χ^2 value obtained from a kinematic fit with the Λ_b^0 candidate constrained to point back to a PV and a mass constraint applied to the J/ψ. In addition, for the signal mode, χ_{c1} or χ_{c2} mass constraints are applied, with the smaller χ^2 values being used; note that this differs from the fit used to separate the mass peaks, which does not include a χ_{c2} constraint. The remaining variables are the p_{T} of the Λ_b^0, proton and kaon, the Λ_b^0 decay-length significance, the cosine of the angle between the momentum of the Λ_b^0 candidate and its displacement from the PV, the proton and kaon χ^2_{IP}, defined as the difference in the vertex-fit χ^2 of the PV when reconstructed with and without the considered particle, and the estimated probabilities that the two muons, kaon and proton, are correctly identified by the particle identification detectors.

Prior to the training, several modifications are made to the simulated samples to better match the kinematic distributions observed in data. First, the simulated $\Lambda_b^0 \to J/\psi p K^-$ events are weighted according to the six-dimensional amplitude model developed in Ref. [4]. Second, a multidimensional gradient-boosting algorithm [36] is used to weight the simulated $\Lambda_b^0 \to J/\psi p K^-$ decays such that the distributions of Λ_b^0 pseudorapidity, the number of tracks in the event, and the GBDT training variables (apart from those related to particle identification) match those observed in the preselected background-subtracted $\Lambda_b^0 \to J/\psi p K^-$ data sample. These weights are also applied to the simulated $\Lambda_b^0 \to \chi_{cJ} p K^-$ samples. Finally, the simulated distributions of the particle identification variables for the muon, proton, and kaon candidates are resampled from data calibration samples ($D^{*+} \to D\pi^+$, $J/\psi \to \mu^+\mu^-$, $\Lambda \to p\pi^-$, and $\Lambda_c^+ \to pK^-\pi^+$ decays) in bins of track p, p_{T} and the number of tracks.

The optimal working point for the GBDT response is chosen by maximizing a figure of merit, $S/\sqrt{S+B}$, where $S = S_0\epsilon$ and B are the expected signal and background yields within ± 20 MeV$/c^2$ of the known Λ_b^0 baryon mass [33], S_0 is the signal yield determined from data without any cut on the GBDT response, and ϵ is the relative efficiency of the GBDT selection, evaluated using the simulated sample. The Λ_b^0 mass sidebands from the data are used to estimate B. The same GBDT and working point are used for the $\Lambda_b^0 \to J/\psi p K^-$ normalization mode. The GBDT selection efficiencies are 78%, 75%, and 68% for the $\Lambda_b^0 \to \chi_{c1} p K^-$, $\Lambda_b^0 \to \chi_{c2} p K^-$, and $\Lambda_b^0 \to J/\psi p K^-$ channels, respectively.

After applying the GBDT requirement, $(2.9 \pm 0.4)\%$ of the selected events contain multiple $\Lambda_b^0 \to \chi_{cJ} p K^-$ candidates. In approximately 80% of these cases, the same $J/\psi p K^-$ combination is combined with an additional, unrelated, photon in the event. The results reported in this Letter retain all candidates and the reported branching fractions are corrected to account for this. The correction factor is 0.993 ± 0.006 (0.986 ± 0.009) for $\Lambda_b^0 \to \chi_{c1} p K^-$ ($\Lambda_b^0 \to \chi_{c2} p K^-$) decays, which is evaluated using a combination of the simulated samples and pseudoexperiments. The larger width of the $\Lambda_b^0 \to \chi_{c2} p K^-$ component leads to the larger uncertainty on the correction factor. For the selected $\Lambda_b^0 \to J/\psi p K^-$ sample, $(0.75 \pm 0.05)\%$ of the events have multiple candidates.

Extended unbinned maximum-likelihood fits are performed to the distributions of $m(\chi_{c1} p K^-)$ and $m(J/\psi p K^-)$ for the signal and normalization modes, respectively. The fit models consist of signal components, each described by the sum of two Crystal Ball (CB) functions [37] with a common mean and power-law tails on both sides, and a linear combinatorial background component. Because of the small $\chi_{c0} \to J/\psi\gamma$ branching fraction [33] the contribution from the χ_{c0} mode is negligible. Several parameters of the signal shapes are determined from fits to simulated samples. These include the tail parameters of the CB functions, the ratio of the widths of the two CB functions, and their relative normalizations. The $\Lambda_b^0 \to \chi_{c2} p K^-$ signal component is shifted to a lower mass in $m(\chi_{c1} p K^-)$ due to the χ_{c1} mass constraint. The signal and background yields, the gradient of the background shape, and the mean of each signal component are free parameters in the fit to data. In addition, the widths of the χ_{c1} and χ_{c2} components in the fit to $m(\chi_{c1} p K^-)$ are allowed to differ from simulation by a common scaling factor, while the width of the narrower CB function in the $\Lambda_b^0 \to J/\psi p K^-$ signal component is a free parameter in the fit to data. The results of these fits are shown in Fig. 2. The measured yields are 453 ± 25, 285 ± 23, and 29815 ± 178 for the χ_{c1}, χ_{c2}, and J/ψ modes, respectively. The significance of each of the signal components in the fit to $m(\chi_{c1} p K^-)$ is calculated using Wilks' theorem [38]. This gives statistical significance of 29 and 17 standard deviations for the decay modes with χ_{c1} and χ_{c2}, respectively.

Simulated samples are used to determine, for each decay mode, the reconstruction and selection efficiency as a function of the Dalitz plot coordinates [39], $m^2(pK^-)$ and $m^2([c\bar{c}]p)$. This approach focuses on the dimensions

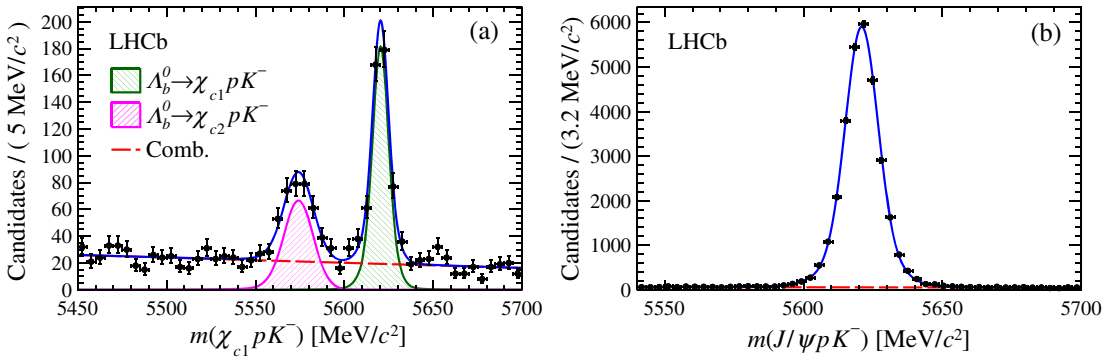

FIG. 2. Fits to the (a) $\Lambda_b^0 \to \chi_{c1} p K^-$ and (b) $\Lambda_b^0 \to J/\psi p K^-$ invariant mass distributions. Data points are shown in black and the results of the fits are shown as solid blue lines. The components are $\Lambda_b^0 \to \chi_{c1} p K^-$ and $\Lambda_b^0 \to \chi_{c2} p K^-$ signal and combinatorial background (Comb.).

where the efficiency variation is expected to be largest whilst averaging over other dimensions in the phase space of $\Lambda_b^0 \to [c\bar{c}]pK^-$ decays. This assumption is treated as a source of systematic uncertainty. The efficiency of each mode, $\epsilon_{[c\bar{c}]}$, is due to geometric acceptance, reconstruction, and selection including the GBDT. The ratios of the phase-space-averaged values of these efficiencies are 0.182 ± 0.005 for $\epsilon_{\chi_{c1}}/\epsilon_{J/\psi}$, and 0.196 ± 0.005 for $\epsilon_{\chi_{c2}}/\epsilon_{J/\psi}$, where the uncertainties are due to the size of the simulated samples. This includes a correction factor for the χ_{cJ} decay modes to account for differences in the photon reconstruction efficiency between data and simulation [20,40].

An efficiency-corrected, background-subtracted yield is determined for each decay mode as $N^{\rm corr}([c\bar{c}]pK^-) = \sum_i w_i/\epsilon_{[c\bar{c}],i}$, where the index i runs over all candidates in the fit range. The w_i are weights determined using the *sPlot* background-subtraction technique [41], which project out the signal component from the combined signal plus background densities using the $[c\bar{c}]pK^-$ invariant mass as a discriminating variable. The corrected yields are found to be about $99\,700 \pm 5300$, $57\,800 \pm 4400$ and $1\,213\,500 \pm 7300$ for the χ_{c1}, χ_{c2}, and J/ψ decay modes, respectively, where the uncertainties are determined from the sum in quadrature of the event weights. Since these weights are determined from a fit in which all shape parameters are fixed, following the *sPlot* prescription, the effect on the yield uncertainty due to the statistical uncertainties on these parameters is not included. To quantify this, the unweighted fit is performed with the shape parameters fixed and then free, and the difference in quadrature of the uncertainties is found to be 1.5% of the yield for $\Lambda_b^0 \to \chi_{c1}pK^-$ decays and 2.1% for $\Lambda_b^0 \to \chi_{c2}pK^-$. A corresponding uncertainty is added in quadrature to that on the efficiency-corrected yield. The effect is negligible for the much larger $\Lambda_b^0 \to J/\psi pK^-$ signal.

The ratios of branching fractions are determined as

$$R_{1(2)} \equiv \frac{\mathcal{B}(\Lambda_b^0 \to \chi_{c1(2)}pK^-)}{\mathcal{B}(\Lambda_b^0 \to J/\psi pK^-)} = \frac{N^{\rm corr}(\chi_{c1(2)}pK^-)}{N^{\rm corr}(J/\psi pK^-)} \times \frac{1}{\mathcal{B}(\chi_{c1(2)} \to J/\psi\gamma)}, \quad (1)$$

$$R_{2/1} \equiv \frac{\mathcal{B}(\Lambda_b^0 \to \chi_{c2}pK^-)}{\mathcal{B}(\Lambda_b^0 \to \chi_{c1}pK^-)} = \frac{N^{\rm corr}(\chi_{c2}pK^-)}{N^{\rm corr}(\chi_{c1}pK^-)} \times \frac{\mathcal{B}(\chi_{c1} \to J/\psi\gamma)}{\mathcal{B}(\chi_{c2} \to J/\psi\gamma)}, \quad (2)$$

where the branching fraction of the $\chi_{c1} \to J/\psi\gamma$ ($\chi_{c2} \to J/\psi\gamma$) decay is taken to be $(33.9 \pm 1.2)\%$ ($(19.2 \pm 0.7)\%$) [33]. Figure 3(a) shows the distribution of $\Delta m + m_{J/\psi}$, where Δm is $m(\mu^+\mu^-\gamma) - m(\mu^+\mu^-)$ and $m_{J/\psi}$ is the known mass of the J/ψ meson [33], while Fig. 3(b) shows $\Delta m + m_{J/\psi}$ for background-subtracted $\Lambda_b^0 \to \chi_{cJ}pK^-$ candidates. Both distributions show clear enhancements at the known masses of the χ_{cJ} mesons.

The $\Lambda_b^0 \to \chi_{cJ}pK^-$ data sample is also used to make a measurement of the Λ_b^0 mass, $m_{\Lambda_b^0}$. The momenta of the particles are scaled to account for known miscalibration of the detector [42]. In addition, the separation between the $\Lambda_b^0 \to \chi_{c1}pK^-$ and $\Lambda_b^0 \to \chi_{c2}pK^-$ components in the $m(\chi_{c1}pK^-)$ spectrum is fixed to the known mass difference between the χ_{c1} and χ_{c2} mesons [33], to obtain a single measurement of $m_{\Lambda_b^0}$ using both decay modes. The mass fit is repeated after these changes, yielding $m_{\Lambda_b^0} = 5619.44 \pm 0.28$ MeV/c^2.

Systematic uncertainties on the ratios of branching fractions are assigned due to imperfect knowledge of the trigger efficiency and data-simulation discrepancies in the photon reconstruction as well as for uncertainties on the corrections applied to the simulated data (kinematic

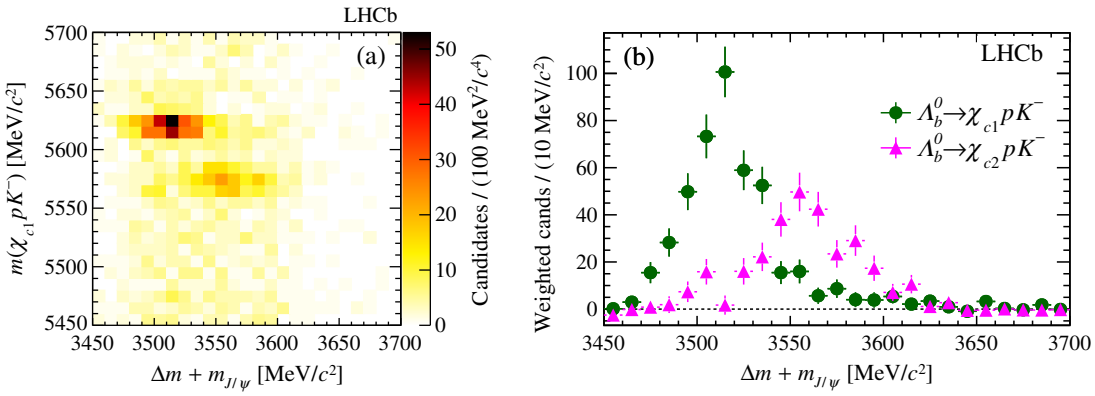

FIG. 3. Distributions of (a) $m(\chi_{c1}pK^-)$ versus $\Delta m + m_{J/\psi}$, where Δm is $m(\mu^+\mu^-\gamma) - m(\mu^+\mu^-)$ and $m_{J/\psi}$ is the known mass of the J/ψ meson [33], and (b) $\Delta m + m_{J/\psi}$ for background-subtracted $\Lambda_b^0 \to \chi_{c1}pK^-$ (green circles) and $\Lambda_b^0 \to \chi_{c2}pK^-$ (magenta triangles) candidates (cands).

reweighting, phase-space weighting, and particle identification resampling), the treatment of multiple candidates, the limited size of simulated data samples, and the models for the signal and background components in the fits. The per-candidate efficiencies as a function of the Dalitz plot coordinates are also replaced by phase-space-averaged efficiencies, and the difference with the nominal result is assigned as a systematic uncertainty.

The systematic uncertainties due to the trigger and photon reconstruction are taken from previous LHCb studies [20,40,43]. The uncertainties assigned due to the kinematic weighting are evaluated by repeating the analysis with alternative efficiency histograms that make use of a simplified three-dimensional weighting procedure with only the Λ_b^0 pseudorapidity, Λ_b^0 p_{T} and event track multiplicity. The uncertainty on the correction for multiple candidates is assigned as a systematic uncertainty. The uncertainty from the size of the simulated samples is determined from pseudoexperiments by varying the efficiency in each bin of each efficiency histogram within its uncertainties. The signal and background components of the invariant mass fits are replaced with the sum of two Gaussian functions and an exponential function, respectively, to estimate systematic uncertainties due to the choice of models.

The largest systematic uncertainties on R_1 and R_2 come from the photon reconstruction (both 4.0%) and kinematic weighting of the simulated samples (2.2% and 2.0%, respectively). For $R_{2/1}$, the largest systematic uncertainties are due to the size of the simulated samples (1.2%) and the treatment of multiple candidates (1.1%). The total systematic uncertainties on R_1, R_2, and $R_{2/1}$ are 5.2%, 5.4%, and 2.0%, respectively.

For the Λ_b^0 mass measurement, systematic uncertainties are assigned due to the uncertainty on the momentum scale for charged-particle tracks, uncertainties on the χ_{cJ} and kaon masses, energy loss in the material, miscalibration of the electromagnetic calorimeter, and the models for the signal and background components in the fit. The total systematic uncertainty (0.26 MeV/c^2) is dominated by the uncertainty on the momentum scale (0.24 MeV/c^2), the effect of which is determined by repeating the analysis with the momentum scaling parameter varied up and down by one standard deviation [42]. The uncertainty from the miscalibration of the electromagnetic calorimeter [44] is found to be small due to the mass constraints that are applied, as is the uncertainty on the energy loss in material, which is taken from a previous LHCb study [45].

In conclusion, the ratios of branching fractions are found to be

$$R_1 = 0.242 \pm 0.014 \pm 0.013 \pm 0.009,$$
$$R_2 = 0.248 \pm 0.020 \pm 0.014 \pm 0.009,$$
$$R_{2/1} = 1.02 \pm 0.10 \pm 0.02 \pm 0.05,$$

where the first uncertainty is statistical, the second systematic, and the third due to the uncertainty on the branching fractions of the $\chi_{cJ} \to J/\psi\gamma$ decays. The values of R_1 and R_2 may be combined with existing measurements of $\mathcal{B}(\Lambda_b^0 \to J/\psi p K^-)/\mathcal{B}(B^0 \to J/\psi K^*(892)^0)$ [46] and $\mathcal{B}(B^0 \to J/\psi K^*(892)^0)$ [47] to obtain absolute branching fraction measurements. As the result in Ref. [47] assumes equal production of B^+B^- and $B^0\bar{B}^0$ pairs at the $\Upsilon(4S)$ resonance, a correction is applied using the current world average value of $\mathcal{B}(\Upsilon(4S) \to B^+B^-)/\mathcal{B}(\Upsilon(4S) \to B^0\bar{B}^0) = 1.058 \pm 0.024$ [33], yielding $\mathcal{B}(B^0 \to J/\psi K^*(892)^0) = (1.22 \pm 0.08) \times 10^{-3}$ and $\mathcal{B}(\Lambda_b^0 \to J/\psi p K^-) = (3.01 \pm 0.21^{+0.43}_{-0.26}) \times 10^{-4}$, where the second uncertainty is due to the ratio of fragmentation fractions, $f_{\Lambda_b^0}/f_d$ [48,49], and the first incorporates all other sources. This gives

$$\mathcal{B}(\Lambda_b^0 \to \chi_{c1} p K^-) = (7.3 \pm 0.4 \pm 0.4 \pm 0.6^{+1.0}_{-0.6}) \times 10^{-5},$$
$$\mathcal{B}(\Lambda_b^0 \to \chi_{c2} p K^-) = (7.5 \pm 0.6 \pm 0.4 \pm 0.6^{+1.1}_{-0.6}) \times 10^{-5},$$

where the third uncertainty is due to uncertainties on the $\chi_{cJ} \to J/\psi\gamma$, $\Lambda_b^0 \to J/\psi p K^-$ and $B^0 \to J/\psi K^*(892)^0$ branching fractions and the fourth is due to $f_{\Lambda_b^0}/f_d$ [48,49]. These results show no suppression of the χ_{c2} mode relative to the χ_{c1} mode in Λ_b^0 baryon decays, which is different to what is observed in $B \to \chi_{cJ} K$ decays [18–20]. These decays will be useful for future investigations into the nature of the two pentaquark candidates observed by the LHCb Collaboration and provide further information on the applicability of the factorization approach in describing b-hadron decays to final states containing charmonium.

The Λ_b^0 mass has also been measured and is found to be $5619.44 \pm 0.28 \pm 0.26$ MeV/c^2, where the first uncertainty is statistical and the second systematic. This result is combined with previous LHCb measurements from $\Lambda_b^0 \to [c\bar{c}]X$ decays [45,50,51] assuming that systematic uncertainties on the momentum scale and energy loss are fully correlated between the measurements while other sources of systematic uncertainties are uncorrelated. The procedure for the combination is the same as that used in Ref. [45]. This yields a new average value of $5619.62 \pm 0.16 \pm 0.13$ MeV/c^2, which supersedes previous combinations of these results.

We express our gratitude to our colleagues in the CERN accelerator departments for the excellent performance of the LHC. We thank the technical and administrative staff at the LHCb institutes. We acknowledge support from CERN and from the national agencies: CAPES, CNPq, FAPERJ and FINEP (Brazil); MOST and NSFC (China); CNRS/IN2P3 (France); BMBF, DFG and MPG (Germany); INFN (Italy); NWO (Netherlands); MNiSW and NCN (Poland); MEN/IFA (Romania); MinES and FASO (Russia); MinECo (Spain); SNSF and SER (Switzerland); NASU (Ukraine); STFC (United Kingdom); NSF (USA). We acknowledge the computing resources that are provided

by CERN, IN2P3 (France), KIT and DESY (Germany), INFN (Italy), SURF (Netherlands), PIC (Spain), GridPP (United Kingdom), RRCKI and Yandex LLC (Russia), CSCS (Switzerland), IFIN-HH (Romania), CBPF (Brazil), PL-GRID (Poland) and OSC (USA). We are indebted to the communities behind the multiple open source software packages on which we depend. Individual groups or members have received support from AvH Foundation (Germany), EPLANET, Marie Skłodowska-Curie Actions and ERC (European Union), Conseil Général de Haute-Savoie, Labex ENIGMASS and OCEVU, Région Auvergne (France), RFBR and Yandex LLC (Russia), GVA, XuntaGal and GENCAT (Spain), Herchel Smith Fund, The Royal Society, Royal Commission for the Exhibition of 1851 and the Leverhulme Trust (United Kingdom).

[1] M. Gell-Mann, A schematic model of baryons and mesons, Phys. Lett. **8**, 214 (1964).
[2] G. Zweig, Report No. CERN-TH-401, 1964.
[3] G. Zweig, CERN-TH-412; reprinted in *Developments in the Quark Theory of Hadrons*, edited by D. Lichtenberg and S. Rosen (Hadronic Press, Nonantum, 1980), Vol. 1, p. 22.
[4] R. Aaij *et al.* (LHCb Collaboration), Observation of $J/\psi p$ Resonances Consistent with Pentaquark States in $\Lambda_b^0 \to J/\psi p K^-$ Decays, Phys. Rev. Lett. **115**, 072001 (2015).
[5] R. Aaij *et al.* (LHCb Collaboration), Model-Independent Evidence for $J/\psi p$ Contributions to $\Lambda_b^0 \to J/\psi p K^-$ Decays, Phys. Rev. Lett. **117**, 082002 (2016).
[6] M. Karliner and J. L. Rosner, New Exotic Meson and Baryon Resonances from Doubly Heavy Hadronic Molecules, Phys. Rev. Lett. **115**, 122001 (2015).
[7] H.-X. Chen, W. Chen, X. Liu, T. G. Steele, and S.-L. Zhu, Towards Exotic Hidden-Charm Pentaquarks in QCD, Phys. Rev. Lett. **115**, 172001 (2015).
[8] L. Roca, J. Nieves, and E. Oset, LHCb pentaquark as a $\bar{D}^*\Sigma_c - \bar{D}^*\Sigma_c^*$ molecular state, Phys. Rev. D **92**, 094003 (2015).
[9] L. Maiani, A. D. Polosa, and V. Riquer, The new pentaquarks in the diquark model, Phys. Lett. B **749**, 289 (2015).
[10] R. F. Lebed, The pentaquark candidates in the dynamical diquark picture, Phys. Lett. B **749**, 454 (2015).
[11] G.-N. Li, X.-G. He, and M. He, Some predictions of diquark model for hidden charm pentaquark discovered at the LHCb, J. High Energy Phys. 12 (2015) 128.
[12] F.-K. Guo, U.-G. Meissner, W. Wang, and Z. Yang, How to reveal the exotic nature of the $P_c(4450)$, Phys. Rev. D **92**, 071502 (2015).
[13] M. Mikhasenko, A triangle singularity and the LHCb pentaquarks, arXiv:1507.06552.
[14] X.-H. Liu, Q. Wang, and Q. Zhao, Understanding the newly observed heavy pentaquark candidates, Phys. Lett. B **757**, 231 (2016).
[15] U.-G. Meissner and J. A. Oller, Testing the $\chi_{c1} p$ composite nature of the $P_c(4450)$, Phys. Lett. B **751**, 59 (2015).
[16] F.-K. Guo, U. G. Meissner, J. Nieves, and Z. Yang, Remarks on the P_c structures and triangle singularities, Eur. Phys. J. A **52**, 318 (2016).
[17] M. Bayar, F. Aceti, F.-K. Guo, and E. Oset, Discussion on triangle singularities in the $\Lambda_b \to J/\psi K^- p$ reaction, Phys. Rev. D **94**, 074039 (2016).
[18] R. Mizuk *et al.* (Belle Collaboration), Observation of two resonance-like structures in the $\pi^+\chi_{c1}$ mass distribution in exclusive $\bar{B}^0 \to K^-\pi^+\chi_{c1}$ decays, Phys. Rev. D **78**, 072004 (2008).
[19] B. Aubert *et al.* (*BABAR* Collaboration), Evidence for $X(3872) \to \psi(2S)\gamma$ in $B^\pm \to X_{3872} K^\pm$ Decays, and a Study of $B \to c\bar{c}\gamma K$, Phys. Rev. Lett. **102**, 132001 (2009).
[20] R. Aaij *et al.* (LHCb Collaboration), Observation of $B_s^0 \to \chi_{c1}\phi$ decay and study of $B^0 \to \chi_{c1,2} K^{*0}$ decays, Nucl. Phys. **B874**, 663 (2013).
[21] M. Beneke and L. Vernazza, $B \to \chi_{cJ} K$ decays revisited, Nucl. Phys. **B811**, 155 (2009).
[22] V. Bhardwaj *et al.* (Belle Collaboration), Inclusive and exclusive measurements of B decays to χ_{c1} and χ_{c2} at Belle, Phys. Rev. D **93**, 052016 (2016).
[23] A. A. Alves Jr. *et al.* (LHCb Collaboration), The LHCb detector at the LHC, J. Instrum. **3**, S08005 (2008).
[24] R. Aaij *et al.* (LHCb Collaboration), LHCb detector performance, Int. J. Mod. Phys. A **30**, 1530022 (2015).
[25] T. Sjöstrand, S. Mrenna, and P. Skands, PYTHIA 6.4 physics and manual, J. High Energy Phys. 05 (2006) 026; T. Sjöstrand, S. Mrenna, and P. Skands, A brief introduction to PYTHIA 8.1, Comput. Phys. Commun. **178**, 852 (2008).
[26] I. Belyaev *et al.*, Handling of the generation of primary events in Gauss, the LHCb simulation framework, J. Phys. Conf. Ser. **331**, 032047 (2011).
[27] D. J. Lange, The EvtGen particle decay simulation package, Nucl. Instrum. Methods Phys. Res., Sect. A **462**, 152 (2001).
[28] P. Golonka and Z. Was, PHOTOS Monte Carlo: A precision tool for QED corrections in Z and W decays, Eur. Phys. J. C **45**, 97 (2006).
[29] J. Allison *et al.* (Geant4 Collaboration), Geant4 developments and applications, IEEE Trans. Nucl. Sci. **53**, 270 (2006); S. Agostinelli *et al.* (Geant4 Collaboration), Geant4: A simulation toolkit, Nucl. Instrum. Methods Phys. Res., Sect. A **506**, 250 (2003).
[30] M. Clemencic, G. Corti, S. Easo, C. R. Jones, S. Miglioranzi, M. Pappagallo, and P. Robbe, The LHCb simulation application, Gauss: Design, evolution and experience, J. Phys. Conf. Ser. **331**, 032023 (2011).
[31] L. Breiman, J. H. Friedman, R. A. Olshen, and C. J. Stone, *Classification and Regression Trees* (Wadsworth International Group, Belmont, CA, 1984).
[32] W. D. Hulsbergen, Decay chain fitting with a Kalman filter, Nucl. Instrum. Methods Phys. Res., Sect. A **552**, 566 (2005).
[33] C. Patrignani *et al.* (Particle Data Group Collaboration), Review of particle physics, Chin. Phys. C **40**, 100001 (2016).
[34] M. Adinolfi *et al.*, Performance of the LHCb RICH detector at the LHC, Eur. Phys. J. C **73**, 2431 (2013).

[35] G. A. Cowan, D. C. Craik, and M. D. Needham, RapidSim: An application for the fast simulation of heavy-quark hadron decays, Comput. Phys. Commun. **214**, 239 (2017).
[36] A. Rogozhnikov, Reweighting with boosted decision trees, J. Phys. Conf. Ser. **762**, 012036 (2016).
[37] T. Skwarnicki, Ph.D. thesis, Institute of Nuclear Physics, Krakow, 1986; Report No. DESY-F31-86-02.
[38] S. S. Wilks, The large-sample distribution of the likelihood ratio for testing composite hypotheses, Ann. Math. Stat. **9**, 60 (1938).
[39] R. H. Dalitz, On the analysis of τ-meson data and the nature of the τ-meson, Philos. Mag. Ser. 5 **44**, 1068 (1953).
[40] E. Govorkova, Study of photon reconstruction efficiency using $B^+ \to J/\psi K^{(*)+}$ decays in the LHCb experiment, Phys. At. Nucl. **79**, 1474 (2016).
[41] M. Pivk and F. R. Le Diberder, sPlot: A statistical tool to unfold data distributions, Nucl. Instrum. Methods Phys. Res., Sect. A **555**, 356 (2005).
[42] R. Aaij *et al.* (LHCb Collaboration), Precision measurement of D meson mass differences, J. High Energy Phys. 06 (2013) 065.
[43] R. Aaij *et al.* (LHCb Collaboration), Measurement of relative branching fractions of B decays to $\psi(2S)$ and J/ψ mesons, Eur. Phys. J. C **72**, 2118 (2012).
[44] I. M. Belyaev, D. Yu. Golubkov, V. Yu. Egorychev, S. M. Polikarpov, and D. V. Savrina, Calibration of the LHCb electromagnetic calorimeter via reconstructing the neutral-pion invariant mass, Phys. At. Nucl. **78**, 1026 (2015).
[45] R. Aaij *et al.* (LHCb Collaboration), Observation of $\Lambda_b^0 \to \psi(2S)pK^-$ and $\Lambda_b^0 \to J/\psi\pi^+\pi^- pK^-$ decays and a measurement of the Λ_b^0 baryon mass, J. High Energy Phys. 05 (2016) 132.
[46] R. Aaij *et al.* (LHCb Collaboration), Study of the productions of Λ_b^0 and $\bar{B}^0$ hadrons in pp collisions and first measurement of the $\Lambda_b^0 \to J/\psi pK^-$ branching fraction, Chin. Phys. C **40**, 011001 (2016).
[47] K. Chilikin *et al.* (Belle Collaboration), Observation of a new charged charmoniumlike state in $\bar{B}^0 \to J/\psi K^-\pi^+$ decays, Phys. Rev. D **90**, 112009 (2014).
[48] R. Aaij *et al.* (LHCb Collaboration), Measurement of b hadron production fractions in 7 TeV pp collisions, Phys. Rev. D **85**, 032008 (2012).
[49] R. Aaij *et al.* (LHCb Collaboration), Study of the kinematic dependences of Λ_b^0 production in pp collisions and a measurement of the $\Lambda_b^0 \to \Lambda_c^+\pi^-$ branching fraction, J. High Energy Phys. 08 (2014) 143.
[50] R. Aaij *et al.* (LHCb Collaboration), Measurement of b-hadron masses, Phys. Lett. B **708**, 241 (2012).
[51] R. Aaij *et al.* (LHCb Collaboration), Measurements of the Λ_b^0, Ξ_b^-, and Ω_b^- Baryon Masses, Phys. Rev. Lett. **110**, 182001 (2013).

R. Aaij,[40] B. Adeva,[39] M. Adinolfi,[48] Z. Ajaltouni,[5] S. Akar,[59] J. Albrecht,[10] F. Alessio,[40] M. Alexander,[53] S. Ali,[43] G. Alkhazov,[31] P. Alvarez Cartelle,[55] A. A. Alves Jr.,[59] S. Amato,[2] S. Amerio,[23] Y. Amhis,[7] L. An,[3] L. Anderlini,[18] G. Andreassi,[41] M. Andreotti,[17,a] J. E. Andrews,[60] R. B. Appleby,[56] F. Archilli,[43] P. d'Argent,[12] J. Arnau Romeu,[6] A. Artamonov,[37] M. Artuso,[61] E. Aslanides,[6] G. Auriemma,[26] M. Baalouch,[5] I. Babuschkin,[56] S. Bachmann,[12] J. J. Back,[50] A. Badalov,[38] C. Baesso,[62] S. Baker,[55] V. Balagura,[7,b] W. Baldini,[17] A. Baranov,[35] R. J. Barlow,[56] C. Barschel,[40] S. Barsuk,[7] W. Barter,[56] F. Baryshnikov,[32] M. Baszczyk,[27,c] V. Batozskaya,[29] V. Battista,[41] A. Bay,[41] L. Beaucourt,[4] J. Beddow,[53] F. Bedeschi,[24] I. Bediaga,[1] A. Beiter,[61] L. J. Bel,[43] V. Bellee,[41] N. Belloli,[21,d] K. Belous,[37] I. Belyaev,[32] E. Ben-Haim,[8] G. Bencivenni,[19] S. Benson,[43] S. Beranek,[9] A. Berezhnoy,[33] R. Bernet,[42] A. Bertolin,[23] C. Betancourt,[42] F. Betti,[15] M.-O. Bettler,[40] M. van Beuzekom,[43] Ia. Bezshyiko,[42] S. Bifani,[47] P. Billoir,[8] A. Birnkraut,[10] A. Bitadze,[56] A. Bizzeti,[18,e] T. Blake,[50] F. Blanc,[41] J. Blouw,[11] S. Blusk,[61] V. Bocci,[26] T. Boettcher,[58] A. Bondar,[36,f] N. Bondar,[31] W. Bonivento,[16] I. Bordyuzhin,[32] A. Borgheresi,[21,d] S. Borghi,[56] M. Borisyak,[35] M. Borsato,[39] F. Bossu,[7] M. Boubdir,[9] T. J. V. Bowcock,[54] E. Bowen,[42] C. Bozzi,[17,40] S. Braun,[12] T. Britton,[61] J. Brodzicka,[56] E. Buchanan,[48] C. Burr,[56] A. Bursche,[16] J. Buytaert,[40] S. Cadeddu,[16] R. Calabrese,[17,a] M. Calvi,[21,d] M. Calvo Gomez,[38,g] A. Camboni,[38] P. Campana,[19] D. H. Campora Perez,[40] L. Capriotti,[56] A. Carbone,[15,h] G. Carboni,[25,i] R. Cardinale,[20,j] A. Cardini,[16] P. Carniti,[21,d] L. Carson,[52] K. Carvalho Akiba,[2] G. Casse,[54] L. Cassina,[21,d] L. Castillo Garcia,[41] M. Cattaneo,[40] G. Cavallero,[20] R. Cenci,[24,k] D. Chamont,[7] M. Charles,[8] Ph. Charpentier,[40] G. Chatzikonstantinidis,[47] M. Chefdeville,[4] S. Chen,[56] S. F. Cheung,[57] V. Chobanova,[39] M. Chrzaszcz,[42,27] A. Chubykin,[31] X. Cid Vidal,[39] G. Ciezarek,[43] P. E. L. Clarke,[52] M. Clemencic,[40] H. V. Cliff,[49] J. Closier,[40] V. Coco,[59] J. Cogan,[6] E. Cogneras,[5] V. Cogoni,[16,l] L. Cojocariu,[30] P. Collins,[40] A. Comerma-Montells,[12] A. Contu,[40] A. Cook,[48] G. Coombs,[40] S. Coquereau,[38] G. Corti,[40] M. Corvo,[17,a] C. M. Costa Sobral,[50] B. Couturier,[40] G. A. Cowan,[52] D. C. Craik,[52] A. Crocombe,[50] M. Cruz Torres,[62] S. Cunliffe,[55] R. Currie,[52] C. D'Ambrosio,[40] F. Da Cunha Marinho,[2] E. Dall'Occo,[43] J. Dalseno,[48] A. Davis,[3] O. De Aguiar Francisco,[54] K. De Bruyn,[6] S. De Capua,[56] M. De Cian,[12] J. M. De Miranda,[1] L. De Paula,[2] M. De Serio,[14,m] P. De Simone,[19] C. T. Dean,[53] D. Decamp,[4] M. Deckenhoff,[10] L. Del Buono,[8] H.-P. Dembinski,[11] M. Demmer,[10] A. Dendek,[28] D. Derkach,[35] O. Deschamps,[5] F. Dettori,[54] B. Dey,[22] A. Di Canto,[40] P. Di Nezza,[19] H. Dijkstra,[40] F. Dordei,[40] M. Dorigo,[41] A. Dosil Suárez,[39]

A. Dovbnya,[45] K. Dreimanis,[54] L. Dufour,[43] G. Dujany,[56] K. Dungs,[40] P. Durante,[40] R. Dzhelyadin,[37] M. Dziewiecki,[12] A. Dziurda,[40] A. Dzyuba,[31] N. Déléage,[4] S. Easo,[51] M. Ebert,[52] U. Egede,[55] V. Egorychev,[32] S. Eidelman,[36,f] S. Eisenhardt,[52] U. Eitschberger,[10] R. Ekelhof,[10] L. Eklund,[53] S. Ely,[61] S. Esen,[12] H. M. Evans,[49] T. Evans,[57] A. Falabella,[15] N. Farley,[47] S. Farry,[54] R. Fay,[54] D. Fazzini,[21,d] D. Ferguson,[52] G. Fernandez,[38] A. Fernandez Prieto,[39] F. Ferrari,[15] F. Ferreira Rodrigues,[2] M. Ferro-Luzzi,[40] S. Filippov,[34] R. A. Fini,[14] M. Fiore,[17,a] M. Fiorini,[17,a] M. Firlej,[28] C. Fitzpatrick,[41] T. Fiutowski,[28] F. Fleuret,[7,n] K. Fohl,[40] M. Fontana,[16,40] F. Fontanelli,[20,j] D. C. Forshaw,[61] R. Forty,[40] V. Franco Lima,[54] M. Frank,[40] C. Frei,[40] J. Fu,[22,o] W. Funk,[40] E. Furfaro,[25,i] C. Färber,[40] E. Gabriel,[52] A. Gallas Torreira,[39] D. Galli,[15,h] S. Gallorini,[23] S. Gambetta,[52] M. Gandelman,[2] P. Gandini,[57] Y. Gao,[3] L. M. Garcia Martin,[69] J. García Pardiñas,[39] J. Garra Tico,[49] L. Garrido,[38] P. J. Garsed,[49] D. Gascon,[38] C. Gaspar,[40] L. Gavardi,[10] G. Gazzoni,[5] D. Gerick,[12] E. Gersabeck,[12] M. Gersabeck,[56] T. Gershon,[50] Ph. Ghez,[4] S. Gianì,[41] V. Gibson,[49] O. G. Girard,[41] L. Giubega,[30] K. Gizdov,[52] V. V. Gligorov,[8] D. Golubkov,[32] A. Golutvin,[55,40] A. Gomes,[1,p] I. V. Gorelov,[33] C. Gotti,[21,d] E. Govorkova,[43] R. Graciani Diaz,[38] L. A. Granado Cardoso,[40] E. Graugés,[38] E. Graverini,[42] G. Graziani,[18] A. Grecu,[30] R. Greim,[9] P. Griffith,[16] L. Grillo,[21,40,d] L. Gruber,[40] B. R. Gruberg Cazon,[57] O. Grünberg,[67] E. Gushchin,[34] Yu. Guz,[37] T. Gys,[40] C. Göbel,[62] T. Hadavizadeh,[57] C. Hadjivasiliou,[5] G. Haefeli,[41] C. Haen,[40] S. C. Haines,[49] B. Hamilton,[60] X. Han,[12] S. Hansmann-Menzemer,[12] N. Harnew,[57] S. T. Harnew,[48] J. Harrison,[56] M. Hatch,[40] J. He,[63] T. Head,[41] A. Heister,[9] K. Hennessy,[54] P. Henrard,[5] L. Henry,[69] E. van Herwijnen,[40] M. Heß,[67] A. Hicheur,[2] D. Hill,[57] C. Hombach,[56] P. H. Hopchev,[41] Z.-C. Huard,[59] W. Hulsbergen,[43] T. Humair,[55] M. Hushchyn,[35] D. Hutchcroft,[54] M. Idzik,[28] P. Ilten,[58] R. Jacobsson,[40] J. Jalocha,[57] E. Jans,[43] A. Jawahery,[60] F. Jiang,[3] M. John,[57] D. Johnson,[40] C. R. Jones,[49] C. Joram,[40] B. Jost,[40] N. Jurik,[57] S. Kandybei,[45] M. Karacson,[40] J. M. Kariuki,[48] S. Karodia,[53] M. Kecke,[12] M. Kelsey,[61] M. Kenzie,[49] T. Ketel,[44] E. Khairullin,[35] B. Khanji,[12] C. Khurewathanakul,[41] T. Kirn,[9] S. Klaver,[56] K. Klimaszewski,[29] T. Klimkovich,[11] S. Koliiev,[46] M. Kolpin,[12] I. Komarov,[41] R. Kopecna,[12] P. Koppenburg,[43] A. Kosmyntseva,[32] S. Kotriakhova,[31] A. Kozachuk,[33] M. Kozeiha,[5] L. Kravchuk,[34] M. Kreps,[50] P. Krokovny,[36,f] F. Kruse,[10] W. Krzemien,[29] W. Kucewicz,[27,c] M. Kucharczyk,[27] V. Kudryavtsev,[36,f] A. K. Kuonen,[41] K. Kurek,[29] T. Kvaratskheliya,[32,40] D. Lacarrere,[40] G. Lafferty,[56] A. Lai,[16] G. Lanfranchi,[19] C. Langenbruch,[9] T. Latham,[50] C. Lazzeroni,[47] R. Le Gac,[6] J. van Leerdam,[43] A. Leflat,[33,40] J. Lefrançois,[7] R. Lefèvre,[5] F. Lemaitre,[40] E. Lemos Cid,[39] O. Leroy,[6] T. Lesiak,[27] B. Leverington,[12] T. Li,[3] Y. Li,[7] Z. Li,[61] T. Likhomanenko,[35,68] R. Lindner,[40] F. Lionetto,[42] X. Liu,[3] D. Loh,[50] I. Longstaff,[53] J. H. Lopes,[2] D. Lucchesi,[23,q] M. Lucio Martinez,[39] H. Luo,[52] A. Lupato,[23] E. Luppi,[17,a] O. Lupton,[40] A. Lusiani,[24] X. Lyu,[63] F. Machefert,[7] F. Maciuc,[30] O. Maev,[31] K. Maguire,[56] S. Malde,[57] A. Malinin,[68] T. Maltsev,[36] G. Manca,[16,l] G. Mancinelli,[6] P. Manning,[61] J. Maratas,[5,r] J. F. Marchand,[4] U. Marconi,[15] C. Marin Benito,[38] M. Marinangeli,[41] P. Marino,[24,k] J. Marks,[12] G. Martellotti,[26] M. Martin,[6] M. Martinelli,[41] D. Martinez Santos,[39] F. Martinez Vidal,[69] D. Martins Tostes,[2] L. M. Massacrier,[7] A. Massafferri,[1] R. Matev,[40] A. Mathad,[50] Z. Mathe,[40] C. Matteuzzi,[21] A. Mauri,[42] E. Maurice,[7,n] B. Maurin,[41] A. Mazurov,[47] M. McCann,[55,40] A. McNab,[56] R. McNulty,[13] B. Meadows,[59] F. Meier,[10] D. Melnychuk,[29] M. Merk,[43] A. Merli,[22,40,o] E. Michielin,[23] D. A. Milanes,[66] M.-N. Minard,[4] D. S. Mitzel,[12] A. Mogini,[8] J. Molina Rodriguez,[1] I. A. Monroy,[66] S. Monteil,[5] M. Morandin,[23] M. J. Morello,[24,k] O. Morgunova,[68] J. Moron,[28] A. B. Morris,[52] A. P. Morris,[52] R. Mountain,[61] F. Muheim,[52] M. Mulder,[43] M. Mussini,[15] D. Müller,[56] J. Müller,[10] K. Müller,[42] V. Müller,[10] P. Naik,[48] T. Nakada,[41] R. Nandakumar,[51] A. Nandi,[57] I. Nasteva,[2] M. Needham,[52] N. Neri,[22,40] S. Neubert,[12] N. Neufeld,[40] M. Neuner,[12] T. D. Nguyen,[41] C. Nguyen-Mau,[41,s] S. Nieswand,[9] R. Niet,[10] N. Nikitin,[33] T. Nikodem,[12] A. Nogay,[68] D. P. O'Hanlon,[50] A. Oblakowska-Mucha,[28] V. Obraztsov,[37] S. Ogilvy,[19] R. Oldeman,[16,l] C. J. G. Onderwater,[70] A. Ossowska,[27] J. M. Otalora Goicochea,[2] P. Owen,[42] A. Oyanguren,[69] P. R. Pais,[41] A. Palano,[14,m] M. Palutan,[19,40] A. Papanestis,[51] M. Pappagallo,[14,m] L. L. Pappalardo,[17,a] C. Pappenheimer,[59] W. Parker,[60] C. Parkes,[56] G. Passaleva,[18] A. Pastore,[14,m] M. Patel,[55] C. Patrignani,[15,h] A. Pearce,[40] A. Pellegrino,[43] G. Penso,[26] M. Pepe Altarelli,[40] S. Perazzini,[40] P. Perret,[5] L. Pescatore,[41] K. Petridis,[48] A. Petrolini,[20,j] A. Petrov,[68] M. Petruzzo,[22,o] E. Picatoste Olloqui,[38] B. Pietrzyk,[4] M. Pikies,[27] D. Pinci,[26] A. Pistone,[20] A. Piucci,[12] V. Placinta,[30] S. Playfer,[52] M. Plo Casasus,[39] T. Poikela,[40] F. Polci,[8] M. Poli Lener,[19] A. Poluektov,[50,36] I. Polyakov,[61] E. Polycarpo,[2] G. J. Pomery,[48] S. Ponce,[40] A. Popov,[37] D. Popov,[11,40] B. Popovici,[30] S. Poslavskii,[37] C. Potterat,[2] E. Price,[48] J. Prisciandaro,[39] C. Prouve,[48] V. Pugatch,[46] A. Puig Navarro,[42] G. Punzi,[24,t] C. Qian,[63] W. Qian,[50] R. Quagliani,[7,48] B. Rachwal,[28] J. H. Rademacker,[48] M. Rama,[24] M. Ramos Pernas,[39] M. S. Rangel,[2] I. Raniuk,[45] F. Ratnikov,[35] G. Raven,[44] M. Ravonel Salzgeber,[40] M. Reboud,[4] F. Redi,[55] S. Reichert,[10] A. C. dos Reis,[1] C. Remon Alepuz,[69] V. Renaudin,[7] S. Ricciardi,[51] S. Richards,[48] M. Rihl,[40] K. Rinnert,[54] V. Rives Molina,[38] P. Robbe,[7] A. B. Rodrigues,[1] E. Rodrigues,[59] J. A. Rodriguez Lopez,[66] P. Rodriguez Perez,[56] A. Rogozhnikov,[35] S. Roiser,[40]

A. Rollings,[57] V. Romanovskiy,[37] A. Romero Vidal,[39] J. W. Ronayne,[13] M. Rotondo,[19] M. S. Rudolph,[61] T. Ruf,[40] P. Ruiz Valls,[69] J. J. Saborido Silva,[39] E. Sadykhov,[32] N. Sagidova,[31] B. Saitta,[16,l] V. Salustino Guimaraes,[1] D. Sanchez Gonzalo,[38] C. Sanchez Mayordomo,[69] B. Sanmartin Sedes,[39] R. Santacesaria,[26] C. Santamarina Rios,[39] M. Santimaria,[19] E. Santovetti,[25,i] A. Sarti,[19,u] C. Satriano,[26,v] A. Satta,[25] D. M. Saunders,[48] D. Savrina,[32,33] S. Schael,[9] M. Schellenberg,[10] M. Schiller,[53] H. Schindler,[40] M. Schlupp,[10] M. Schmelling,[11] T. Schmelzer,[10] B. Schmidt,[40] O. Schneider,[41] A. Schopper,[40] H. F. Schreiner,[59] K. Schubert,[10] M. Schubiger,[41] M.-H. Schune,[7] R. Schwemmer,[40] B. Sciascia,[19] A. Sciubba,[26,u] A. Semennikov,[32] A. Sergi,[47] N. Serra,[42] J. Serrano,[6] L. Sestini,[23] P. Seyfert,[21] M. Shapkin,[37] I. Shapoval,[45] Y. Shcheglov,[31] T. Shears,[54] L. Shekhtman,[36,f] V. Shevchenko,[68] B. G. Siddi,[17,40] R. Silva Coutinho,[42] L. Silva de Oliveira,[2] G. Simi,[23,q] S. Simone,[14,m] M. Sirendi,[49] N. Skidmore,[48] T. Skwarnicki,[61] E. Smith,[55] I. T. Smith,[52] J. Smith,[49] M. Smith,[55] l. Soares Lavra,[1] M. D. Sokoloff,[59] F. J. P. Soler,[53] B. Souza De Paula,[2] B. Spaan,[10] P. Spradlin,[53] S. Sridharan,[40] F. Stagni,[40] M. Stahl,[12] S. Stahl,[40] P. Stefko,[41] S. Stefkova,[55] O. Steinkamp,[42] S. Stemmle,[12] O. Stenyakin,[37] H. Stevens,[10] S. Stoica,[30] S. Stone,[61] B. Storaci,[42] S. Stracka,[24,t] M. E. Stramaglia,[41] M. Straticiuc,[30] U. Straumann,[42] L. Sun,[64] W. Sutcliffe,[55] K. Swientek,[28] V. Syropoulos,[44] M. Szczekowski,[29] T. Szumlak,[28] S. T'Jampens,[4] A. Tayduganov,[6] T. Tekampe,[10] G. Tellarini,[17,a] F. Teubert,[40] E. Thomas,[40] J. van Tilburg,[43] M. J. Tilley,[55] V. Tisserand,[4] M. Tobin,[41] S. Tolk,[49] L. Tomassetti,[17,a] D. Tonelli,[24] S. Topp-Joergensen,[57] F. Toriello,[61] R. Tourinho Jadallah Aoude,[1] E. Tournefier,[4] S. Tourneur,[41] K. Trabelsi,[41] M. Traill,[53] M. T. Tran,[41] M. Tresch,[42] A. Trisovic,[40] A. Tsaregorodtsev,[6] P. Tsopelas,[43] A. Tully,[49] N. Tuning,[43] A. Ukleja,[29] A. Ustyuzhanin,[35] U. Uwer,[12] C. Vacca,[16,l] V. Vagnoni,[15,40] A. Valassi,[40] S. Valat,[40] G. Valenti,[15] R. Vazquez Gomez,[19] P. Vazquez Regueiro,[39] S. Vecchi,[17] M. van Veghel,[43] J. J. Velthuis,[48] M. Veltri,[18,w] G. Veneziano,[57] A. Venkateswaran,[61] T. A. Verlage,[9] M. Vernet,[5] M. Vesterinen,[12] J. V. Viana Barbosa,[40] B. Viaud,[7] D. Vieira,[63] M. Vieites Diaz,[39] H. Viemann,[67] X. Vilasis-Cardona,[38,g] M. Vitti,[49] V. Volkov,[33] A. Vollhardt,[42] B. Voneki,[40] A. Vorobyev,[31] V. Vorobyev,[36,f] C. Voß,[9] J. A. de Vries,[43] C. Vázquez Sierra,[39] R. Waldi,[67] C. Wallace,[50] R. Wallace,[13] J. Walsh,[24] J. Wang,[61] D. R. Ward,[49] H. M. Wark,[54] N. K. Watson,[47] D. Websdale,[55] A. Weiden,[42] M. Whitehead,[40] J. Wicht,[50] G. Wilkinson,[57,40] M. Wilkinson,[61] M. Williams,[40] M. P. Williams,[47] M. Williams,[58] T. Williams,[47] F. F. Wilson,[51] J. Wimberley,[60] M. A. Winn,[7] J. Wishahi,[10] W. Wislicki,[29] M. Witek,[27] G. Wormser,[7] S. A. Wotton,[49] K. Wraight,[53] K. Wyllie,[40] Y. Xie,[65] Z. Xu,[4] Z. Yang,[3] Z. Yang,[60] Y. Yao,[61] H. Yin,[65] J. Yu,[65] X. Yuan,[61] O. Yushchenko,[37] K. A. Zarebski,[47] M. Zavertyaev,[11,b] L. Zhang,[3] Y. Zhang,[7] A. Zhelezov,[12] Y. Zheng,[63] X. Zhu,[3] V. Zhukov,[33] J. B. Zonneveld,[52] and S. Zucchelli[15]

(LHCb Collaboration)

[1]*Centro Brasileiro de Pesquisas Físicas (CBPF), Rio de Janeiro, Brazil*
[2]*Universidade Federal do Rio de Janeiro (UFRJ), Rio de Janeiro, Brazil*
[3]*Center for High Energy Physics, Tsinghua University, Beijing, China*
[4]*LAPP, Université Savoie Mont-Blanc, CNRS/IN2P3, Annecy-Le-Vieux, France*
[5]*Clermont Université, Université Blaise Pascal, CNRS/IN2P3, LPC, Clermont-Ferrand, France*
[6]*CPPM, Aix-Marseille Université, CNRS/IN2P3, Marseille, France*
[7]*LAL, Université Paris-Sud, CNRS/IN2P3, Orsay, France*
[8]*LPNHE, Université Pierre et Marie Curie, Université Paris Diderot, CNRS/IN2P3, Paris, France*
[9]*I. Physikalisches Institut, RWTH Aachen University, Aachen, Germany*
[10]*Fakultät Physik, Technische Universität Dortmund, Dortmund, Germany*
[11]*Max-Planck-Institut für Kernphysik (MPIK), Heidelberg, Germany*
[12]*Physikalisches Institut, Ruprecht-Karls-Universität Heidelberg, Heidelberg, Germany*
[13]*School of Physics, University College Dublin, Dublin, Ireland*
[14]*Sezione INFN di Bari, Bari, Italy*
[15]*Sezione INFN di Bologna, Bologna, Italy*
[16]*Sezione INFN di Cagliari, Cagliari, Italy*
[17]*Sezione INFN di Ferrara, Ferrara, Italy*
[18]*Sezione INFN di Firenze, Firenze, Italy*
[19]*Laboratori Nazionali dell'INFN di Frascati, Frascati, Italy*
[20]*Sezione INFN di Genova, Genova, Italy*
[21]*Sezione INFN di Milano Bicocca, Milano, Italy*
[22]*Sezione INFN di Milano, Milano, Italy*

[23]Sezione INFN di Padova, Padova, Italy
[24]Sezione INFN di Pisa, Pisa, Italy
[25]Sezione INFN di Roma Tor Vergata, Roma, Italy
[26]Sezione INFN di Roma La Sapienza, Roma, Italy
[27]Henryk Niewodniczanski Institute of Nuclear Physics Polish Academy of Sciences, Kraków, Poland
[28]AGH - University of Science and Technology, Faculty of Physics and Applied Computer Science, Kraków, Poland
[29]National Center for Nuclear Research (NCBJ), Warsaw, Poland
[30]Horia Hulubei National Institute of Physics and Nuclear Engineering, Bucharest-Magurele, Romania
[31]Petersburg Nuclear Physics Institute (PNPI), Gatchina, Russia
[32]Institute of Theoretical and Experimental Physics (ITEP), Moscow, Russia
[33]Institute of Nuclear Physics, Moscow State University (SINP MSU), Moscow, Russia
[34]Institute for Nuclear Research of the Russian Academy of Sciences (INR RAN), Moscow, Russia
[35]Yandex School of Data Analysis, Moscow, Russia
[36]Budker Institute of Nuclear Physics (SB RAS), Novosibirsk, Russia
[37]Institute for High Energy Physics (IHEP), Protvino, Russia
[38]ICCUB, Universitat de Barcelona, Barcelona, Spain
[39]Universidad de Santiago de Compostela, Santiago de Compostela, Spain
[40]European Organization for Nuclear Research (CERN), Geneva, Switzerland
[41]Institute of Physics, Ecole Polytechnique Fédérale de Lausanne (EPFL), Lausanne, Switzerland
[42]Physik-Institut, Universität Zürich, Zürich, Switzerland
[43]Nikhef National Institute for Subatomic Physics, Amsterdam, The Netherlands
[44]Nikhef National Institute for Subatomic Physics and VU University Amsterdam, Amsterdam, The Netherlands
[45]NSC Kharkiv Institute of Physics and Technology (NSC KIPT), Kharkiv, Ukraine
[46]Institute for Nuclear Research of the National Academy of Sciences (KINR), Kyiv, Ukraine
[47]University of Birmingham, Birmingham, United Kingdom
[48]H.H. Wills Physics Laboratory, University of Bristol, Bristol, United Kingdom
[49]Cavendish Laboratory, University of Cambridge, Cambridge, United Kingdom
[50]Department of Physics, University of Warwick, Coventry, United Kingdom
[51]STFC Rutherford Appleton Laboratory, Didcot, United Kingdom
[52]School of Physics and Astronomy, University of Edinburgh, Edinburgh, United Kingdom
[53]School of Physics and Astronomy, University of Glasgow, Glasgow, United Kingdom
[54]Oliver Lodge Laboratory, University of Liverpool, Liverpool, United Kingdom
[55]Imperial College London, London, United Kingdom
[56]School of Physics and Astronomy, University of Manchester, Manchester, United Kingdom
[57]Department of Physics, University of Oxford, Oxford, United Kingdom
[58]Massachusetts Institute of Technology, Cambridge, Massachusetts, USA
[59]University of Cincinnati, Cincinnati, Ohio, USA
[60]University of Maryland, College Park, Maryland, USA
[61]Syracuse University, Syracuse, New York, USA
[62]Pontifícia Universidade Católica do Rio de Janeiro (PUC-Rio), Rio de Janeiro, Brazil
(associated with Institution Universidade Federal do Rio de Janeiro (UFRJ), Rio de Janeiro, Brazil)
[63]University of Chinese Academy of Sciences, Beijing, China
(associated with Institution Center for High Energy Physics, Tsinghua University, Beijing, China)
[64]School of Physics and Technology, Wuhan University, Wuhan, China
(associated with Institution Center for High Energy Physics, Tsinghua University, Beijing, China)
[65]Institute of Particle Physics, Central China Normal University, Wuhan, Hubei, China
(associated with Institution Center for High Energy Physics, Tsinghua University, Beijing, China)
[66]Departamento de Fisica, Universidad Nacional de Colombia, Bogota, Colombia
(associated with Institution LPNHE, Université Pierre et Marie Curie, Université Paris Diderot, CNRS/IN2P3, Paris, France)
[67]Institut für Physik, Universität Rostock, Rostock, Germany
(associated with Institution Physikalisches Institut, Ruprecht-Karls-Universität Heidelberg, Heidelberg, Germany)
[68]National Research Centre Kurchatov Institute, Moscow, Russia
(associated with Institution Institute of Theoretical and Experimental Physics (ITEP), Moscow, Russia)
[69]Instituto de Fisica Corpuscular, Centro Mixto Universidad de Valencia - CSIC, Valencia, Spain
(associated with Institution ICCUB, Universitat de Barcelona, Barcelona, Spain)
[70]Van Swinderen Institute, University of Groningen, Groningen, The Netherlands
(associated with Institution Nikhef National Institute for Subatomic Physics, Amsterdam, The Netherlands)

[a]Also at Università di Ferrara, Ferrara, Italy.
[b]Also at P.N. Lebedev Physical Institute, Russian Academy of Science (LPI RAS), Moscow, Russia.

[c]Also at AGH - University of Science and Technology, Faculty of Computer Science, Electronics and Telecommunications, Kraków, Poland.
[d]Also at Università di Milano Bicocca, Milano, Italy.
[e]Also at Università di Modena e Reggio Emilia, Modena, Italy.
[f]Also at Novosibirsk State University, Novosibirsk, Russia.
[g]Also at LIFAELS, La Salle, Universitat Ramon Llull, Barcelona, Spain.
[h]Also at Università di Bologna, Bologna, Italy.
[i]Also at Università di Roma Tor Vergata, Roma, Italy.
[j]Also at Università di Genova, Genova, Italy.
[k]Also at Scuola Normale Superiore, Pisa, Italy.
[l]Also at Università di Cagliari, Cagliari, Italy.
[m]Also at Università di Bari, Bari, Italy.
[n]Also at Laboratoire Leprince-Ringuet, Palaiseau, France.
[o]Also at Università degli Studi di Milano, Milano, Italy.
[p]Also at Universidade Federal do Triângulo Mineiro (UFTM), Uberaba-MG, Brazil.
[q]Also at Università di Padova, Padova, Italy.
[r]Also at Iligan Institute of Technology (IIT), Iligan, Philippines.
[s]Also at Hanoi University of Science, Hanoi, Viet Nam.
[t]Also at Università di Pisa, Pisa, Italy.
[u]Also at Università di Roma La Sapienza, Roma, Italy.
[v]Also at Università della Basilicata, Potenza, Italy.
[w]Also at Università di Urbino, Urbino, Italy.